Role of the mass asymmetry of reaction on the geometry of vanishing flow.

Supriya Goyal

Department of Physics, Panjab University, Chandigarh 160 014, India

Abstract

We study the transverse flow throughout the mass asymmetry range as a function of the impact parameter, keeping the total mass of the system fixed. We find that the geometry of vanishing flow (GVF) i.e. the impact parameter at which flow vanishes and its mass dependence is quite sensitive to the mass asymmetry of the reaction. With increase in the mass asymmetry, the value of GVF decreases, while its mass dependence increases. Our results indicate the sizable role of mass asymmetry on GVF as on balance energy.

Keywords: heavy-ion collisions, quantum molecular dynamics (QMD) model, balance energy, mass asymmetric reactions, impact parameter, geometry of vanishing flow

1. Introduction

Reaction dynamics at low incident energies is mainly governed by attractive mean field which prompts the emission of particles into the backward hemisphere, whereas at higher incident energies, due to the dominance of repulsive binary nucleon-nucleon (nn) collisions, particle emission takes place into the forward hemisphere. While going from the low to higher incident energies, the in-plane flow of particles, also known as collective transverse flow, disappears at a particular energy. This particular value of energy is called the Energy of Vanishing Flow (EVF) or alternatively, the Balance Energy (E_{bal}) [1, 2, 3, 4, 5, 6, 7, 8, 9, 10]. Extensive investigations have been

Email address: `supriyagoyal.pu@gmail.com,ashuphysics@gmail.com` (Supriya Goyal)

done to calculate the accurate value of E_{bal} in the last 2-3 decades, both experimentally as well as theoretically [1, 2, 3, 4, 5, 6, 7, 8, 9, 10].

The balance energy is found to be very sensitive towards the nuclear matter equation of state, nn cross-section [2, 3, 4, 5, 6, 7, 8, 9, 10], size of the system [4], impact parameter [2, 5, 7, 9, 10], mass asymmetry of the reaction [11] and incident energy of the projectile [12]. The mass dependence of balance energy is found to obey the power law behavior ($\propto A_{TOT}^{\tau}$; where A_{TOT} is the mass of projectile+mass of target) and τ = -1/3 has been reported in the literature [4], whereas recent attempts suggested a deviation from the above mentioned power law [6, 7, 8].

In one of the recent studies, Goyal and Puri [11] found for the first time, the role of the mass asymmetry of reaction (defined as $\eta = A_T - A_p/A_T + A_P$; where A_T and A_P are the masses of the target and projectile, respectively) on E_{bal} and its mass dependence. It has been found that almost independent of the system mass as well as impact parameter, for large asymmetries ($\eta = 0.7$), the effect of asymmetry can be 15% with momentum dependent interactions.

It is well mentioned in the literature that the E_{bal} increases approximately linearly as a function of impact parameter for symmetric reactions ($\eta = 0$). The linear behavior depends upon the nuclear equation of state [13], mass of the system [13] as well as the mass asymmetry [14]. From the isolated studies with symmetric systems, it has been found that linear behavior of E_{bal} with colliding geometry decreases with increase in system mass [13, 14, 15]. For the mass asymmetric systems, the effect of colliding geometries on the E_{bal} is found for the first time by Goyal [14]. It has been predicted that the linear dependence of E_{bal} on colliding geometries increases with increase in mass asymmetry for each fixed mass of the system.

In a recent study by Puri *et al.* [16], it has been found for the first time that while going from perfectly central collisions to most peripheral ones, the collective transverse flow passes through a maximum (at low values of impact parameter), a zero value (at some intermediate value of impact parameter), and achieves negative values (at large values of impact parameter), at a fixed incident energy. The intermediate value of impact parameter where collective transverse flow vanishes is termed as Geometry of Vanishing Flow (GVF) [16]. It has been found that mass dependence of GVF is insensitive to the nuclear matter equation of state and momentum dependent interactions, whereas it is quite sensitive to the binary nn cross-section [16]. It is noted that the study was done only for the symmetric systems. Therefore, in the present study we aim to find the role of mass asymmetry on the GVF at a fixed

value of energy. The present calculations are done with Quantum Molecular Dynamics (QMD) model [17], which is found to explain the experimental results of the mass and impact parameter dependence of the balance energy (for symmetric systems) very nicely [8]. The model is explained in Section II. Results and discussion are explained in Section III and finally we summarizes the results in Section IV.

2. The quantum molecular dynamics model

The quantum molecular dynamics model (QMD) is a n-body theory and simulates the reaction on an event by event basis [17]. The explicit two and three-body interactions in the model, preserves the fluctuations and correlations which are important for N-body phenomenon such as multifragmentation [17].

In QMD model, each nucleon α is represented by a Gaussian wave packet with a width of $\sqrt{L}$ centered around the mean position $\vec{r}_\alpha$(t) and mean momentum $\vec{p}_\alpha$(t) [17]:

$$\phi_\alpha(\vec{r}, \vec{p}, t) = \frac{1}{(2\pi L)^{3/4}} e^{\left[-\{\vec{r}-\vec{r}_\alpha(t)\}^2/4L\right]} e^{[i\vec{p}_\alpha(t)\cdot\vec{r}/\hbar]}. \tag{1}$$

The Wigner distribution of a system with $A_T + A_P$ nucleons is given by

$$f(\vec{r}, \vec{p}, t) = \sum_{\alpha=1}^{A_T+A_P} \frac{1}{(\pi\hbar)^3} e^{\left[-\{\vec{r}-\vec{r}_\alpha(t)\}^2/2L\right]} e^{\left[-\{\vec{p}-\vec{p}_\alpha(t)\}^2 2L/\hbar^2\right]'}, \tag{2}$$

with L = 1.08 fm^2.

The center of each Gaussian (in the coordinate and momentum space) is chosen by the Monte Carlo procedure. The momentum of nucleons (in each nucleus) is chosen between zero and local Fermi momentum [$= \sqrt{2m_\alpha V_\alpha(\vec{r})}$; $V_\alpha(\vec{r})$ is the potential energy of nucleon α]. Naturally, one has to take care that the nuclei, thus generated, have right binding energy and proper root mean square radii.

The centroid of each wave packet is propagated using the classical equations of motion [17]:

$$\frac{d\vec{r}_\alpha}{dt} = \frac{dH}{d\vec{p}_\alpha}, \tag{3}$$

$$\frac{d\vec{p}_\alpha}{dt} = -\frac{dH}{d\vec{r}_\alpha}, \tag{4}$$

where the Hamiltonian is given by

$$H = \sum_{\alpha} \frac{\vec{p}_{\alpha}^{2}}{2m_{\alpha}} + V^{tot}. \tag{5}$$

Our total interaction potential V^{tot} reads as [17]

$$V^{tot} = V^{Loc} + V^{Yuk} + V^{Coul} + V^{MDI}, \tag{6}$$

with

$$V^{Loc} = t_1\delta(\vec{r}_\alpha - \vec{r}_\beta) + t_2\delta(\vec{r}_\alpha - \vec{r}_\beta)\delta(\vec{r}_\alpha - \vec{r}_\gamma), \tag{7}$$

$$V^{Yuk} = t_3 e^{-|\vec{r}_\alpha - \vec{r}_\beta|/m} / \left(|\vec{r}_\alpha - \vec{r}_\beta|/m\right), \tag{8}$$

with m = 1.5 fm and t_3 = -6.66 MeV.

The static (local) Skyrme interaction can further be parametrized as:

$$U^{Loc} = \alpha\left(\frac{\rho}{\rho_o}\right) + \beta\left(\frac{\rho}{\rho_o}\right)^{\gamma}. \tag{9}$$

Here α, β and γ are the parameters that define equation of state. The momentum dependent interaction is obtained by parameterizing the momentum dependence of the real part of the optical potential. The final form of the potential reads as

$$U^{MDI} \approx t_4 ln^2[t_5(\vec{p}_\alpha - \vec{p}_\beta)^2 + 1]\delta(\vec{r}_\alpha - \vec{r}_\beta). \tag{10}$$

Here t_4 = 1.57 MeV and t_5 = 5 $\times 10^{-4} MeV^{-2}$. A parameterized form of the local plus momentum dependent interaction (MDI) potential (at zero temperature) is given by

$$U = \alpha\left(\frac{\rho}{\rho_0}\right) + \beta\left(\frac{\rho}{\rho_0}\right) + \delta ln^2[\epsilon(\rho/\rho_0)^{2/3} + 1]\rho/\rho_0. \tag{11}$$

The parameters α, β, and γ in above Eq. (11) must be readjusted in the presence of momentum dependent interactions so as to reproduce the ground state properties of the nuclear matter. The set of parameters corresponding to different equations of state can be found in Ref. [17].

3. Results and discussion

For the present study, we simulated the reactions of ${}^{20}_{10}Ne+^{20}_{10}Ne$ ($\eta = 0$), ${}^{17}_{8}O+^{23}_{11}Na$ ($\eta = 0.1$), ${}^{14}_{7}N+^{26}_{12}Mg$ ($\eta = 0.3$), ${}^{10}_{5}B+^{30}_{14}Si$ ($\eta = 0.5$), ${}^{6}_{3}Li+^{34}_{16}S$ ($\eta = 0.7$), and ${}^{3}_{2}He+^{37}_{17}Cl$ ($\eta = 0.9$), for $A_{TOT} = 40$, ${}^{40}_{20}Ca+^{40}_{20}Ca$ ($\eta = 0$), ${}^{36}_{18}Ar+^{44}_{20}Ca$ ($\eta = 0.1$), ${}^{28}_{14}Si+^{52}_{24}Cr$ ($\eta = 0.3$), ${}^{20}_{10}Ne+^{60}_{28}Ni$ ($\eta = 0.5$), ${}^{10}_{5}B+^{70}_{32}Ge$ ($\eta = 0.7$), and ${}^{6}_{3}Li+^{74}_{34}Se$ ($\eta = 0.9$), for $A_{TOT} = 80$, ${}^{80}_{36}Kr+^{80}_{36}Kr$ ($\eta = 0$), ${}^{70}_{32}Ge+^{90}_{40}Zr$ ($\eta = 0.1$), ${}^{54}_{26}Fe+^{106}_{48}Cd$ ($\eta = 0.3$), ${}^{40}_{20}Ca+^{120}_{52}Te$ ($\eta = 0.5$), ${}^{24}_{12}Mg+^{136}_{58}Ce$ ($\eta = 0.7$), and ${}^{6}_{3}Li+^{154}_{64}Gd$ ($\eta = 0.9$), for $A_{TOT} = 160$, and ${}^{120}_{52}Te+^{120}_{52}Te$ ($\eta = 0$), ${}^{108}_{48}Cd+^{132}_{56}Ba$ ($\eta = 0.1$), ${}^{84}_{38}Sr+^{156}_{66}Dy$ ($\eta = 0.3$), ${}^{60}_{28}Ni+^{180}_{74}W$ ($\eta = 0.5$), ${}^{36}_{18}Ar+^{204}_{82}Pb$ ($\eta = 0.7$), and ${}^{7}_{3}Li+^{233}_{92}U$ ($\eta = 0.9$), for $A_{TOT} = 240$ at full range of colliding geometries ranging from the central to peripheral collisions in small steps of 0.25 and at a fixed incident energy of 200 MeV/nucleon. We have varied η from 0 to 0.9 for every system mass A_{TOT} =40, 80, 160, and 240. Soft equation of state with momentum dependent interaction (SMD) is used along with energy dependent Cugnon cross-section.

To calculate the E_{bal}, we use *directed transverse momentum* $< P_x^{dir} >$, which is defined as:

$$\langle P_x^{dir} \rangle = \frac{1}{A} \sum_i \text{sign}\{Y(i)\} \; \mathbf{p}_x(i), \tag{12}$$

where $Y(i)$ and $\mathbf{p}_x(i)$ are the rapidity distribution and transverse momentum of i^{th} particle, respectively.

In Fig. 1, we display the $< P_x^{dir} >$ as a function of reduced impact parameter (b/b_{max}; where b_{max} = radius of projectile + radius of target) for η = 0 - 0.9. The study is done for different mass ranges. All reactions are followed till 200 fm/c, where $< P_x^{dir} >$ saturates. Symbols are explained in the caption of the figure. Lines are just to guide the eye. As expected, in all cases i.e. for all values of η and A_{TOT}, $< P_x^{dir} >$ first increases with b/b_{max}, reaches a maximal value and after passing through a zero at some intermediate value of impact parameter, attains negative values at large $b/bmax$. The trend is uniform throughout the mass asymmetry range i.e. from η = 0-0.9 for every A_{TOT}. The value of GVF (impact parameter at which $< P_x^{dir} >$ attains a zero) varies with η and A_{TOT}. For lighter systems and larger η, the value of GVF is small compared to the heavier systems and smaller η.

In Fig. 2, we display GVF as a function of η for A_{TOT} = 40, 80, 160, and 240. Symbols are explained in the caption of the figure. Lines are just to guide the eye. The percentage variation in GVF while going from $\eta = 0$ to

0.9 is -62%, -42.03%, -40.91%, and -21.21%, respectively for A_{TOT} = 40, 80, 160, and 240. The negative signs indicates that GVF decreases with increase in η. It is very clear from the figure that with increase in system mass, the effect of mass asymmetry of the reaction on GVF decreases. The effect is similar to as predicted for E_{bal} [11]. It is well known that with increase in η and impact parameter, the E_{bal} increases while with increase in A_{TOT}, E_{bal} decreases. This is due to the decrease in nn collisions with increase in η and impact parameter, and increase in Coulomb repulsion with increase in A_{TOT}. The present study has been done at fixed incident lab energy, therefore, the effective center-of-mass energy also decreases as η increases for every fixed system mass. To compensate all these factors, the value of impact parameter, where flow vanishes, decreases as η increases.

In Fig. 3, we display GVF as a function of A_{TOT} for each η. Symbols are explained in the caption of the figure. Lines are power law fits ($\propto A^{\tau}_{TOT}$). The percentage variation in GVF while going from A_{TOT} = 40 to 240 is 98%, 94.12%, 104.17%, 121.43%, 174.19%, and 310.53%, respectively, for η = 0, 0.1, 0.3, 0.5, 0.7, and 0.9. This shows that the dependence of GVF on system mass increases with increase in η. We also display the results of $Hard^{40}$, HMD^{40}, SMD^{40}, and SMD^{cug} for symmetric systems with total mass ranging from 80 to 262 and at an incident energy of 150 MeV/nucleon. Values are taken from Ref. [16]. Superscripts represents the values of the cross-sections.

From the value of GVF for $\eta = 0$, at 200 MeV/nucleon and 150 MeV/nucleon using SMD^{cug} equation of state, we found that GVF depends on the incident energy. It was found in Ref. [16] that mass dependence of GVF is very sensitive to in-medium nn cross-section. From the figure, it is clear that the difference in the value of GVF due to the change in cross-section i.e. between $SMD^{cug}(\eta = 0)$ and $SMD^{40}(\eta = 0)$ at 150 MeV/nucleon is same as between $SMD^{cug}(\eta = 0, E = 150 MeV/nucleon)$ and $SMD^{cug}(\eta = 0, E = 200 MeV/nucleon)$. Very interestingly, it shows that for symmetric systems, GVF is equally sensitive to nn cross-section and incident energy.

In Fig. 4, we display the value of τ as a function of η. Symbols are explained in the caption of the figure. Line is just to guide the eye. The value of τ increases with increase in η. For $\eta = 0$, the values of τ at 150 MeV/nucleon are 0.24±0.01, 0.23±0.02, 0.25±0.01, and 0.44±0.02, respectively, for $Hard^{40}$, HMD^{40}, SMD^{40}, and SMD^{cug} equations of state and are displayed in the figure [16]. The difference in values of τ at $\eta = 0$ is due to the variation of incident energy and mass range for which τ is calculated

[16].

In Fig. 5, we display the mean field ($< P_x^{dir} >_{mf}$) and binary nn collision ($< P_x^{dir} >_{coll}$) contribution of total ($< P_x^{dir} >$) as a function of the colliding geometry. As expected, ($< P_x^{dir} >_{coll}$) is always positive and ($< P_x^{dir} >_{mf}$) is always negative for all colliding geometries. The shaded areas cover the full range of mass in the present study i.e. from 40 to 240. Upper(lower) boundary of the shaded area for $\eta = 0$ represent heavier(lighter) mass, while for $\eta = 0.9$, the upper boundary of ($< P_x^{dir} >_{mf}$) represent heavier mass and of ($< P_x^{dir} >_{coll}$) represents lighter mass. For different η, the effect of mean field and binary collisions is different for different masses at and around respective GVF, thus making GVF and its mass dependence quite sensitive to mass asymmetry.

4. Summary

In short, we have studied the collective transverse flow throughout the mass asymmetry range $\eta = 0$ - 0.9, as a function of impact parameter. Study is done for different mass ranges. We found that the geometry of vanishing flow (GVF) is quite sensitive to the mass asymmetry. For each η, the mass dependence of GVF follows a power law behavior and dependence on the system mass increases with increase in η. The present study concludes that mass asymmetry has a significant role on the geometry of vanishing flow.

5. Acknowledgement

Author is thankful to Dr. Rajeev K. Puri for interesting and constructive discussions. This work is supported by a research grant from the Council of Scientific and Industrial Research (CSIR), Govt. of India, vide grant No. 09/135(0563)/2009-EMR-1.

References

[1] D. Krofcheck *et al.*, Phys. Rev. Lett. 63 (1989) 2028.

[2] J. Lukasik *et al.*, Phys. Lett. B 608 (2005) 223.

[3] V. de la Mota, F. Sebille, M. Farine, B. Remaud, P. Schuck, Phys. Rev. C 46 (1992) 677;
D. Cussol *et al.*, Phys. Rev. C 65 (2002) 044604;

H. Zhou, Z. Li, Y. Zhuo, Phys. Rev. C 50 (1994) R2664;
H. Zhou, Z. Li, Y. Zhuo, G. Mao, Nucl. Phys. A 580 (1994) 627.

[4] G. D. Westfall *et al.*, Phys. Rev. Lett. 71 (1993) 1986.

[5] R. Pak *et al.*, Phys. Rev. C 53 (1996) R1469.

[6] D. J. Magestro *et al.*, Phys. Rev. C 61 (2000) 021602(R);
S. Soff, C. Hartnack, H. Stöcker, W. Greiner, Phys. Rev. C 51 (1995) 3320.

[7] D. J. Magestro, W. Bauer, G. D. Westfall, Phys. Rev. C 62 (2000) 041603(R).

[8] A. D. Sood and R. K. Puri, Phys. Rev. C 69 (2004) 054612;
A. D. Sood and R. K. Puri, Phys. Rev. C 73 (2006) 067602;
A. D. Sood and R. K. Puri, Phys. Lett. B 594 (2004) 260;
A. D. Sood and R. K. Puri, Eur. Phys. J. A 30 (2006) 571.

[9] J. P. Sullivan *et al.*, Phys. Lett. B 249 (1990) 8.

[10] A. Buta *et al.*, Nucl. Phys. A 584 (1995) 397.

[11] S. Goyal and R. K. Puri, Nucl. Phys. A 853 (2011) 164.

[12] B. Hong *et al.*, Phys. Rev. C 66 (2000) 034901.

[13] R. Chugh and R. K. Puri, Phys. Rev. C 82 (2010) 014603.

[14] S. Goyal, Phys. Rev. C (2011) - submitted.

[15] R. Chugh and R. K. Puri, Int. J. Mod. Phys. E 19 (2010) 2009.

[16] R. Chugh and A. D. Sood, arXiv:1010.1120v2 (2011).

[17] J. Aichelin, Phys. Rep. 202 (1991) 233.

Figure Captions

FIG. 1. (Color online) $< P_x^{dir} >$ (MeV/c) as a function of reduced impact parameter (b/b_{max}) for different system masses. The results for different mass asymmetries η = 0, 0.1, 0.3, 0.5, 0.7, and 0.9 are represented, respectively, by the solid squares, circles, triangles, inverted triangles, diamonds, and stars. Results are at an incident energy of 200 MeV/nucleon.

FIG. 2. (Color online) The geometry of vanishing flow (GVF) as a function of η for different system masses. The results for different system masses (A_{TOT}) = 40, 80, 160, and 240 are represented, respectively, by the half filled squares, circles, triangles, and inverted triangles.

FIG. 3. (Color online) The geometry of vanishing flow (GVF) as a function of system mass. The results for different mass asymmetries η = 0, 0.1, 0.3, 0.5, 0.7, and 0.9 are represented, respectively, by the solid squares, circles, triangles, inverted triangles, diamonds, and stars. Lines are the power law fits. The values of GVF at 150 MeV/nucleon and η=0 are represented by open circles, triangles, inverted triangles, and diamonds, respectively for $Hard^{40}$, HMD^{40}, SMD^{40}, and SMD^{cug} equations of state [16].

FIG. 4. (Color online) The value of τ as a function of η. The result of present study is shown by open squares. Open circles, triangles, inverted triangles, and diamonds, represents the value of τ, respectively for $Hard^{40}$, HMD^{40}, SMD^{40}, and SMD^{cug} equations of state at 150 MeV/nucleon [16].

FIG. 5. (Color online) The decomposition of $< P_x^{dir} >$ into mean and binary collision parts as a function of the reduced impact parameter for different mass asymmetries (η = 0 and 0.9).

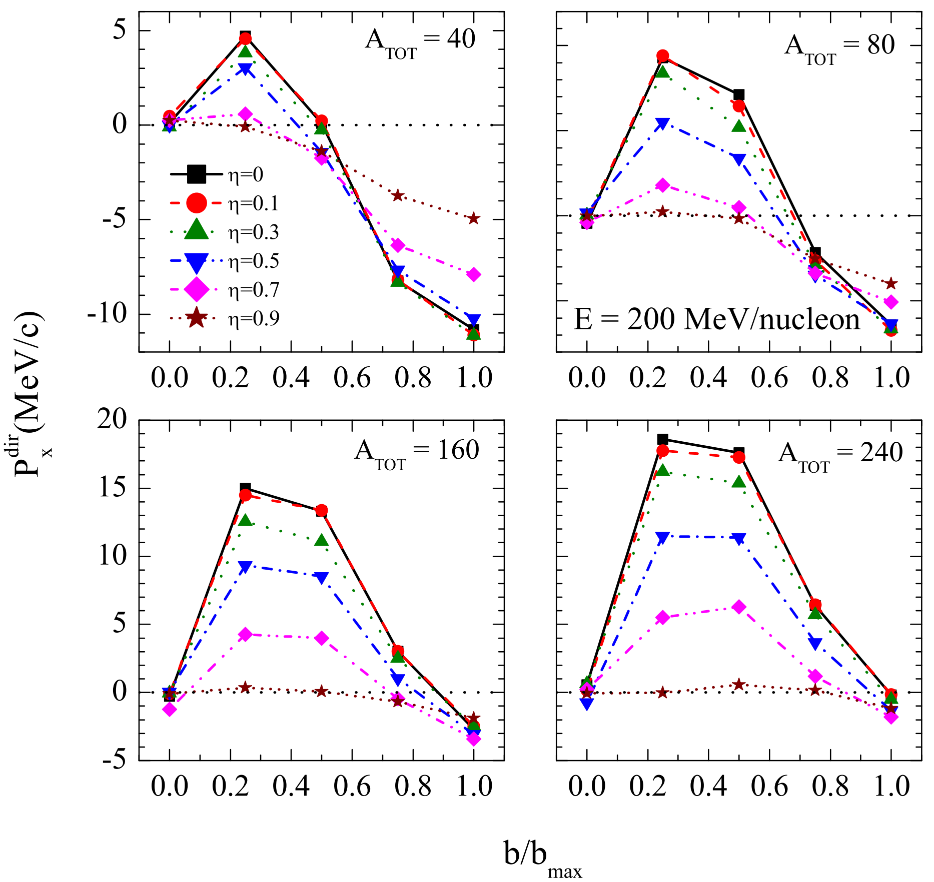

A_{TOT} = 40
A_{TOT} = 80
A_{TOT} = 160
A_{TOT} = 240
E = 200 MeV/nucleon
η=0
η=0.1
η=0.3
η=0.5
η=0.7
η=0.9
P_x^{dir}(MeV/c)
b/b_{max}

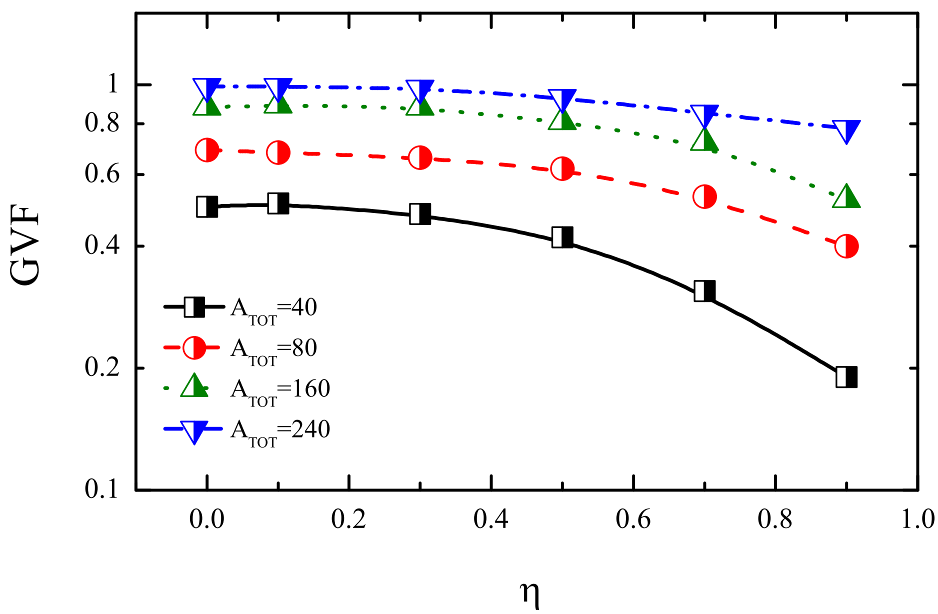
GVF
η
0.1
0.2
0.4
0.6
0.8
1
0.0
0.2
0.4
0.6
0.8
1.0
A_TOT=40
A_TOT=80
A_TOT=160
A_TOT=240

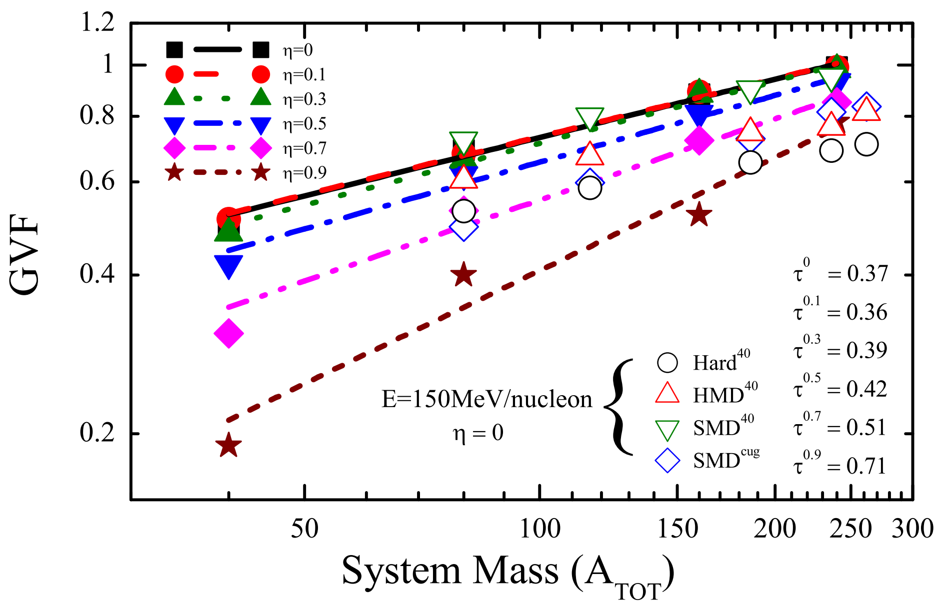

GVF
System Mass (A_{TOT})
η=0
η=0.1
η=0.3
η=0.5
η=0.7
η=0.9
E=150MeV/nucleon
η = 0
Hard^{40}
HMD^{40}
SMD^{40}
SMD^{cug}
$\tau^{0} = 0.37$
$\tau^{0.1} = 0.36$
$\tau^{0.3} = 0.39$
$\tau^{0.5} = 0.42$
$\tau^{0.7} = 0.51$
$\tau^{0.9} = 0.71$

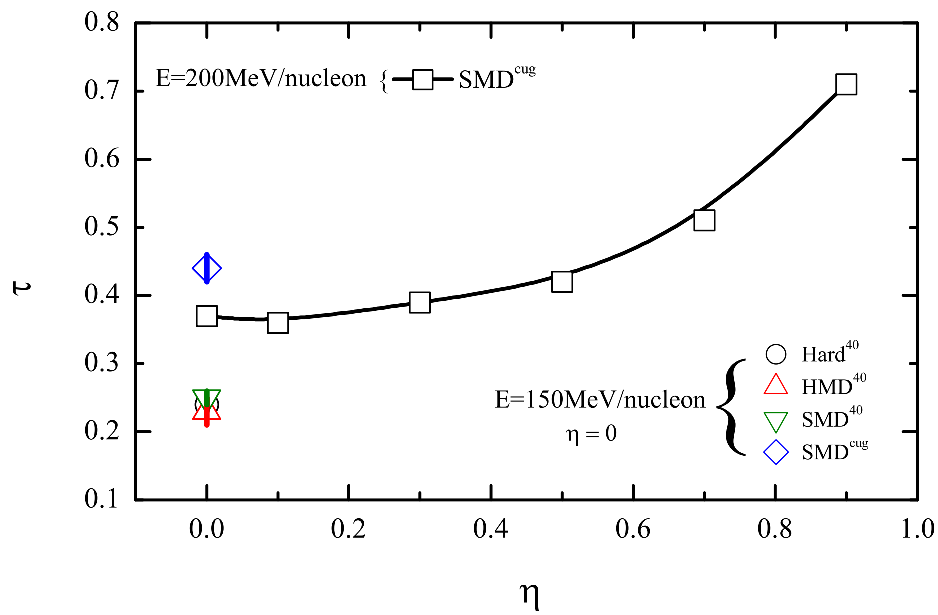
E=200MeV/nucleon { SMD^cug
E=150MeV/nucleon
η = 0
Hard^40
HMD^40
SMD^40
SMD^cug
τ
η
0.8
0.7
0.6
0.5
0.4
0.3
0.2
0.1
0.0
0.2
0.4
0.6
0.8
1.0

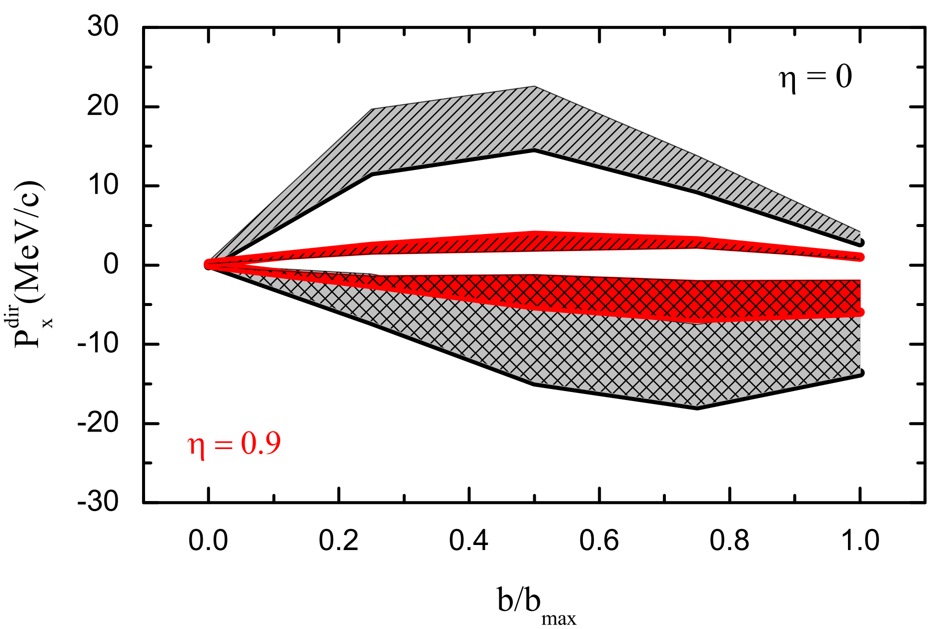

30
20
10
0
-10
-20
-30
P_x^{dir}(MeV/c)
$\eta = 0$
$\eta = 0.9$
0.0
0.2
0.4
0.6
0.8
1.0
b/b_{max}